Mass Spectrometry Imaging of Two Neocortical Areas Reveals the Histological Selectivity of Schizophrenia-Associated Lipid Alterations

Применение метода масс-спектрометрической визуализации двух областей неокортекса для выявления гистологической селективности липидных изменений, характерных при шизофрении

doi: 10.17816/CP15488

Original research

Maria Osetrova[1], Marina Zavolskova[1], Pavel Mazin[2], Elena Stekolschikova[1], Gleb Vladimirov[1], Olga Efimova[1], Anna Morozova[3,4], Yana Zorkina[3,4], Denis Andreyuk[3], George Kostyuk[3], Evgeniy Nikolaev[1], Philipp Khaitovich[1]

[1] Skolkovo Institute of Science and Technology, Moscow, Russia

[2] Wellcome Sanger Institute, Hinxton, UK

[3] Mental-health clinic No. 1 named after N.A. Alexeev, Moscow, Russia

[4] V. Serbsky National Medical Research Centre of Psychiatry and Narcology of the Ministry of Health of the Russian Federation, Moscow, Russia

Мария Осетрова[1], Марина Завольскова[1], Павел Мазин[2], Елена Стекольщикова[1], Глеб Владимиров[1], Ольга Ефимова[1], Анна Морозова[3,4], Яна Зоркина[3,4], Денис Андреюк[3], Георгий Костюк[3], Евгений Николаев[1], Филипп Хайтович[1]

[1] АНОО ВО «Сколковский институт науки и технологий», Москва, Россия

[2] Институт Сенгера, Хинкстон, Великобритания

[3] ГБУЗ «Психиатрическая клиническая больница № 1 им. Н.А. Алексеева Департамента здравоохранения города Москвы», Москва, Россия

[4] ФГБУ «Национальный медицинский исследовательский центр психиатрии и наркологии им. В.П. Сербского» Минздрава России, Москва, Россия

ABSTRACT

BACKGROUND: Schizophrenia is a psychiatric disorder known to affect brain structure and functionality. Structural changes in the brain at the level of gross anatomical structures have been fairly well studied, while microstructural changes, especially those associated with changes in the molecular composition of the brain, are still being investigated. Of special interest are lipids and metabolites, for which some previous studies have shown association with schizophrenia.

AIM: To utilize a spatially resolved analysis of the brain lipidome composition to investigate the degree and nature of schizophrenia-associated lipidome alterations in the gray and white matter structures of two neocortical regions — the dorsolateral prefrontal cortex (Brodmann area 9, BA9) and the posterior part of the superior temporal gyrus (Brodmann area 22, posterior part, BA22p), as well compare the distribution of the changes between the two regions and tissue types.

METHODS: We employed Matrix-Assisted Laser Desorption/Ionization Mass Spectrometric Imaging (MALDI-MSI), supplemented by a statistical analysis, to examine the lipid composition of brain sections. A total of 24 neocortical sections from schizophrenia patients (*n*=2) and a healthy control group (*n*=2), representing the two aforementioned neocortical areas, were studied, yielding data for 131 lipid compounds measured across more than a million MALDI-MSI pixels.

RESULTS: Our findings revealed an uneven distribution of schizophrenia-related lipid alterations across the two neocortical regions. The BA22p showed double the differences in its subcortical white matter structures compared to BA9, while less bias was detected in the gray matter layers. While the schizophrenia-associated lipid differences generally showed good agreement between brain regions at the lipid class level for both gray and white matter, there were consistently more discrepancies for white matter structures.

CONCLUSION: Our study found a consistent yet differential association of schizophrenia with the brain lipidome composition of distinct neocortical areas, particularly subcortical white matter. These findings highlight the need for broader brain coverage in future schizophrenia research and underscore the potential of spatially resolved molecular analysis methods in identifying structure-specific effects.

АННОТАЦИЯ

ВВЕДЕНИЕ: Шизофрения — это психическое расстройство, известное своим влиянием на структуру и функциональность мозга. Хотя изменения в архитектуре мозга на уровне крупных анатомических структур были исследованы достаточно подробно, микроструктурные изменения, особенно связанные с молекулярным составом мозга, остаются предметом интенсивного изучения. В последние годы особое внимание уделяется липидам и метаболитам, поскольку ряд предыдущих работ выявил их возможную связь с шизофренией. Понимание этих молекулярных изменений может помочь в раскрытии механизмов, лежащих в основе этого расстройства, и в разработке новых подходов к его диагностике и лечению.

ЦЕЛЬ: Исследовать степень и характер ассоциированных с шизофренией различий в пространственном распределении липидов в сером и белом веществе двух областей неокортекса — в дорсолатеральной префронтальной коре (область Бродмана 9, BA9) и задней части верхней височной извилины (область Бродмана 22, задняя часть, BA22p), а также сравнить распределение различий между двумя областями и типами тканей.

МЕТОДЫ: Проведена визуализация при помощи метода масс-спектрометрии с применением матрично-активированной лазерной десорбции/ионизации (MALDI-MSI). Всего было исследовано 24 среза, полученных от больных шизофренией (*n*=2) и от здорового контроля (*n*=2), представляющих две вышеупомянутых области неокортекса, что позволило проанализировать данные по 131 липидному соединению, измеренному по более чем миллиону пикселей MALDI-MSI.

РЕЗУЛЬТАТЫ: Обнаружено неоднородное распределение разницы в уровне липидов, связанных с шизофренией, в двух исследованных областях неокортекса. Белое вещество из BA22p показало больше различий по сравнению с белым веществом из BA9, в то время как в сером веществе дисбаланс количества различий менее выражен. Хотя изменения липидов, связанные с шизофренией, в целом, хорошо согласуются между областями мозга на уровне классов липидов как для серого, так и для белого вещества, было обнаружено значительно больше расхождений для структур белого вещества.

ЗАКЛЮЧЕНИЕ: Исследование выявило согласованную, но дифференцированную связь между шизофренией и составом липидома мозга в различных областях неокортекса, особенно в подкорковом белом веществе. Полученные результаты подчеркивают важность учета специфики мозговых структур в будущих исследованиях

шизофрении и демонстрируют перспективность методов молекулярного анализа с пространственным разрешением для выявления структурно-ориентированных изменений, связанных с этим расстройством.

Keywords: *schizophrenia; lipidomics; mass-spectrometry; MALDI-MSI; neocortex*
Ключевые слова: *шизофрения; липидом; масс-спектрометрия; MALDI-MSI; неокортекс*

INTRODUCTION

Schizophrenia is a psychiatric disorder affecting 0.3 to 0.45% of the global population[1] [1, 2] and up to 4.7% in selected countries [3, 4], with a significant social and healthcare impact [2]. The molecular underpinnings of schizophrenia remain poorly understood due to the multifactorial nature of the disease and brain tissue heterogeneity. Recent advances in high-resolution molecular imaging techniques, such as Matrix-Assisted Laser Desorption/Ionization Mass Spectrometry Imaging (MALDI-MSI), offer unprecedented opportunities to elucidate the spatial distribution of molecules on tissue sections [5–7], thereby enabling a more comprehensive understanding of the biochemical changes associated with schizophrenia [8]. Studying molecular changes in other disorders using MALDI-MSI provides a powerful approach to identifying and localizing potential biomarkers [9], in an effort towards a better understanding of disease etiology [10, 11].

Previous studies using mass spectrometry have indicated the presence of detectable metabolic alterations in the brains of schizophrenia patients: particularly in hydrophobic metabolites known as lipids [12–14]. Similarly, genetic studies have revealed associations linked to the genes involved in lipid metabolism in schizophrenia patients [15, 16]. Despite an increase in studies that investigate the metabolome, specifically the lipidome, of the schizophrenia brain, a comprehensive understanding of the metabolic alterations associated with this debilitating disorder is yet to be achieved. One reason for this lack of systemic understanding is the near-exclusive focus of most molecular studies on a specific brain area — the dorsolateral prefrontal cortex.

Another contributing factor to incomplete understanding of schizophrenia-associated alterations is the lack of spatial resolution in most of the methods used for molecular tissue examination. Traditional lipidomic studies often prepare samples for liquid or gas chromatography, combined with mass spectrometry, by homogenizing the biological sample, which often results in a loss of information about the lipids' spatial distribution. At the same time, the cerebral cortex possesses a complex multilayer structure that influences its functionality [17, 18]. Moreover, certain lipids and lipid classes have been shown to exhibit a distinctive spatial distribution within the cortex layers [19]. Collectively, these points underscore the need to employ methods that incorporate spatial resolution in order to examine the molecular composition of multiple brain regions in a schizophrenia brain, which has not been implemented previously.

The dorsolateral prefrontal cortex, which has been the focus of multiple schizophrenia studies, was associated with such negative symptoms as affected cognitive control [20], working memory dysfunction [21], and anhedonia [22–24]. Investigation of the spatial lipidome of the prefrontal cortex of schizophrenia has indicated some abnormalities in phospholipids but yielded limited data on other lipid classes. It also lacked statistical evaluations [8]. Variations in the volume of the left-side superior temporal gyrus have been consistently associated with auditory hallucinations, which are a primary positive symptom of schizophrenia [25]. Furthermore, gene expression studies that have examined multiple neocortical regions have reported the greatest number of gene expression alterations in this area [26–28]. However, no previous studies have focused on the spatial distribution of the lipids in this temporal region. Moreover, no comparative analysis has been conducted for the two regions.

Our study aimed to utilize a spatially resolved analysis of the brain lipidome composition to investigate the degree and nature of schizophrenia-associated lipidome alterations in the gray and white matter structure [27–29] of two neocortical regions — the dorsolateral prefrontal cortex (Brodmann area 9, BA9) and the posterior part of the superior temporal gyrus (Brodmann area 22, posterior part, BA22p). The focus on these two regions made it possible to establish a reference frame for the results obtained in the form of the well-studied region BA9, as well as the

[1] Available from: https://www.who.int/news-room/fact-sheets/detail/schizophrenia

opportunity to collect completely new data for a region that had not previously been studied using our chosen method. We further examined two histological areas within each region — one corresponding to subcortical white matter and the other to neocortical gray matter layers.

METHODS

Tissue samples

Healthy control (HC) and schizophrenia patient (SZ) brain samples (sex: M/F=0/2 and 1/1; age: 36, 63 and 62, 56; respectively) were obtained from the biospecimens of the contract research organization National BioService (Saint Petersburg, Russia). No subject in the control group had a history of psychiatric or neurodegenerative disease and no gross anatomical abnormalities were revealed during the pathoanatomical assessment. Brain donors were diagnosed with schizophrenia according to ICD-10 by psychiatrists during inpatient treatment at Mental-health clinic No. 1 named after N.A. Alexeev (Moscow, Russia). Each subject suffered sudden death with no prolonged agony state.

All the post-mortem brain samples were sectioned, placed on aluminum blocks, and frozen on dry ice. All sample transport was conducted on dry ice and long-term storage in –80°C freezers. There was no sample thawing or heating at any point. The two regions of interest (BA9 and BA22p) were located according to the Atlas of the Human Brain[2] by a neuroanatomist. A total of 24 samples were dissected. They covered two regions from two individuals from both the HC and SZ and were measured in three replicates, meaning that each region in each individual was represented by three brain tissue slices (Table S1 in the Supplementary).

Tissue preparation

The brain samples were sectioned using the Leica CM1950 microtome cryostat (Leica Biosystems, China). Cutting was done at a chamber temperature of –18°C; sample temperature was –15°C. The thickness of the sections was set to 20 µm. The sections were placed on an ITO (indium tin oxide) coated glass slide without an adhesive medium (Hudson Surface Technology, Glass Slides for MALDI imaging, Republic of Korea) and attached to the glass by thaw-mounting. The sections were next placed in a desiccator for 90 minutes. Air was removed from the chamber using a MEMVAK 2x1 membrane pump to a 30-mbar pressure at room temperature. A solution of α-cyano-4-hydroxycinnamic acid (Sigma-Aldrich, USA), with a concentration of 5 mg/mL in a 50/50 water/acetonitrile mixture with 0.1% and trifluoroacetic acid (TFA, Sigma-Aldrich, USA), was diluted twice. No internal standards were added. The diluted solution was sprayed using an Iwata Micron CM-B2 airbrush (Anest Iwata, Japan) for two seconds and allowed to dry for 2.5 minutes. This process was repeated 20 times.

MALDI experiment

MALDI images were obtained using a modified MALDI-Orbitrap mass spectrometer (Thermo Scientific Q-Exactive Orbitrap with MALDI/ESI Injector from Spectroglyph, LLC, USA) equipped with an 355 nm Nd:YAG Laser Garnet (Laser-export. Co. Ltd, Russia). For positive ion induction the laser power was set to a 20 J repetition rate to 1.7 kHz. The distance between the sample on a coordinate table and ion funnel was 0.5 cm. The produced ions were captured by ion funnel and transferred to a Q-Exactive Orbitrap mass spectrometer (Thermo). Mass-spectra were obtained in a mass range of m/z 500–1000, and the mass resolution was 140,000. No fragmentation was carried out. The scanning pattern was left-right. MALDI interface operated in the MALDI mode at a laser repetition rate of 1 kHz. The ion accumulation time per pixel was 250 ms. The tissue region to be imaged and the raster step size were controlled using the Spectroglyph MALDI Injector Software. No oversampling was performed. To generate images, the spectra were collected at 40-µm intervals in both the *x* and *y* dimensions across the surface of the sample. Ion images were generated from raw files (obtained from the Orbitrap tune software) and coordinate files (obtained from the MALDI Injector Software) by the Image Insight software from Spectroglyph LLC. MALDI raw mass spectra were converted to *.ibd and *.imzML formats using the Spectroglyph software, with the background noise threshold set to zero. All further processing was done using Cardinal 2.8.0 (Kylie A. Bemis, USA), an R package designed for mass spectrometry imaging data analysis [30].

For image analysis, duplicated coordinates were removed from the converted files. Peak intensity was evaluated as height, then the spectra were normalized by the total

[2] Acronym: A91. Name: lateral subdivision of area 9 [Internet]. [cited 2023 Dec 7]. Available from: https://atlas.brain-map.org/atlas?atlas=265297126#atlas=265297121023399 58&structure=10179&x=30131.805555555555&y=37587.999131944445&zoom=-7&resolution=138. 6&plate=71&z=3

ion current. We performed peak picking on the basis of a signal-to-noise ratio threshold equal to three to select peak centers for the downstream analysis. The signal-to-noise ratio was calculated based on the difference between the mean peak height in a window of predefined size and the mean height in a window of the manually selected flat part of the spectrum [31]. After the peak picking procedure, the spectra of each pixel were aligned to the average spectrum of the entire image, in accordance with the library functionality Cardinal 2.8.0 (Kylie A. Bemis, USA). Peaks present in less than 7% of the sample spectra were removed from further analysis. Images were generated with the peaks of interest centered around the measured m/z values.

Peaks originating from the glass slide surface not covered by tissue and uninformative parts of the spectra containing no biologically relevant peaks were removed from each sample spectral data. To do that, the sample image area was divided into two parts using the spatial k-means algorithm; one of the clusters corresponding to the tissue sample, the other — to the sample-free matrix-covered surface of the glass slide. The mapping of the clusters to the sample and the surrounding area was manually curated by visual inspection of the slides. Mean feature intensities were calculated for the two clusters, and only peaks with 1.5 times greater mean intensities within the sample cluster compared to the surrounding sample-free area were kept. After these filtration steps, all sample spectra were aligned to the spectrum with the largest number of detected peaks.

For the clustering of pixels within the sample area into white and gray matter clusters, histological staining of the adjacent sample sections was used. Unsupervised clustering of gray matter (without preliminary peaks selection) was performed with the spatial Shrunken Centroids function from the Cardinal library. The following parameters were used: s=1, k=3, r=1, where s is the sparsity parameters, k is the number of clusters, and r is the smoothing radius.

Peaks annotation

The peaks were annotated as lipid species based on their mass-to-charge ratio with the mass difference threshold between the data and target values set to 20 ppm. For cases of multiple matches, the following rules were applied (also see Figure S1 in the Supplementary).

One peak — one lipid — one adduct. When a unique match occurred between the lipid annotation of a particular adduct and the m/z ratio in MALDI, this annotation was assigned to the MALDI peak.

Several peaks — one lipid — different adducts. If peaks with masses matching the same lipid were detected in MALDI but with different adducts, priority was given to annotating the lipid with a hydrogen adduct. If no hydrogen adduct was present, the sodium adduct took higher priority over the potassium adduct.

One peak — several lipids — different adducts. If one MALDI peak corresponded to the annotation of two different lipids, where one had a hydrogen adduct and the other had any other adduct, the peak was assigned with annotation of a lipid with a hydrogen adduct.

One peak — several lipids — one adduct. If one MALDI peak corresponded to the annotation of two different lipids, both of which contained a hydrogen adduct, the peak was assigned the annotation of both lipids.

The remaining lipids coincided with lipid classes characteristic of a given tissue and matrix [32–35][3].

Histology of sections

The histology of the white and gray matter on the brain sections was revealed by luxol fast blue staining (blue color for lipid-rich compartments) and by eosin (pink color for protein-rich cytoplasm). Brain sections were briefly defated to increase dye penetration: they were placed gradually in ethyl alcohol (50%, 75%, 95% and 100%) and back to 95% for 1 min in each solution. Then, the sections were left in a 0.1% luxol fast blue solution (BioOptica, Italy) in ethyl alcohol with 0.5% glacial acetic acid in a 56°C oven for 12–14 h. Excess stain was rinsed off with 95% ethyl alcohol and then in distilled water. Staining was differentiated in a 0.05% lithium carbonate solution (BioOptica, Italy) in water for 30 seconds and rinsed in distilled water several times, with constant control by microscopic examination if gray matter was clear and white matter sharply defined. Then, the sections were counterstained with a 1% eosin solution (BioVitrum, Russia) in water for 30–40 seconds, rinsed in distilled water, dehydrated briefly in IsoPrep (BioVitrum, Russia), cleared in Bio Clear (Bio-Optica, Italy), and coverslipped with Bio Mount HM (Bio-Optica, Italy). Histology images were acquired with a Zeiss Axio.Observer. Z1 (ZEISS, Germany) transmitted light microscope system.

[3] Bemis K. Cardianl peakPick [Internet]. [cited 2023 Dec 7]. Available from: https://github.com/kuwisdelu/Cardinal/blob/devel/R/process2-peakPick.R

Statistical analysis

Before performing statistical tests for the MALDI-MSI data, an image with lipids, intersected with González et. al [19] work, was generated, where the intensity of both lipids (PC 40:6 and SM d42:2) was normalized in 0 to 1 range. To explore the differences in the PC 40:6 lipid between the disease and control in each of the obtained layers in gray matter for both of the explored regions, intensities were normalized within layers for each region in a base-two log scale, followed by ANOVA between layers for each region and the disease.

All statistical tests were performed on base-two log transformed measured intensities. Mean values were calculated for gray matter and white matter clusters in each slide. Measured intensities from three replicates and all individuals in each group were averaged for further analysis. The difference (for base-two log transformed values) between the schizophrenia and control group was calculated for each lipid species within each region (BA9 and BA22p) and each histological cluster (gray matter and white matter). Groups of lipids with changes between the two groups were defined as having absolute changes of 0.25

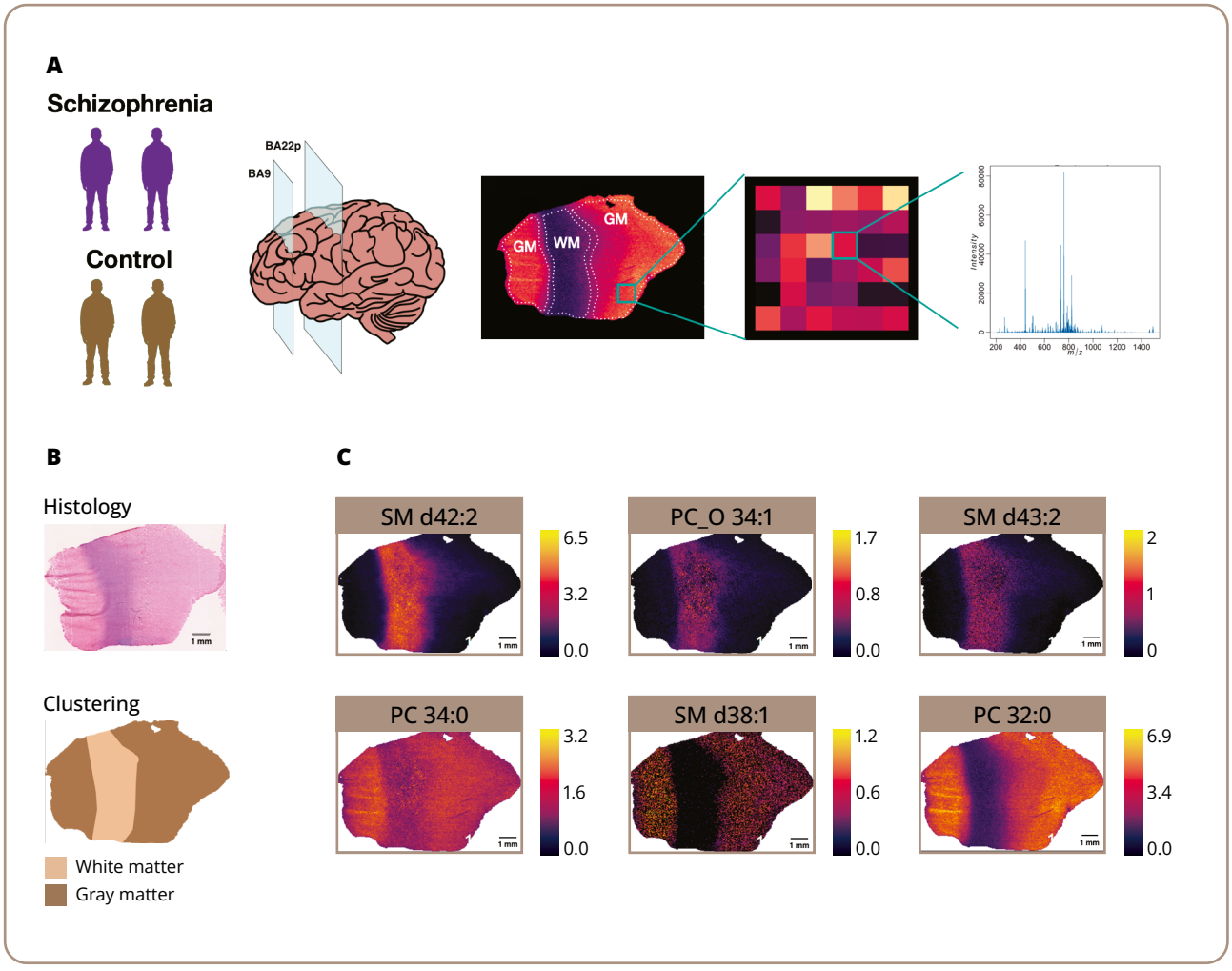

Figure 1. Application of the MALDI-MSI method to brain region analysis.

Note: (A) A schematic representation of the sample analysis. From left to right: sample set, thin sections dissection from two brain regions (BA9 and BA22p), and spatial distribution of the intensity levels of a particular mass spectrometric peak, representing a specific molecular ion, measured as a portion of a mass spectrogram collected for each pixel of the tissue section. (B) Histological staining and MALDI-MSI signal-based clustering of the pixels of one of the 24 examined neocortical sections. (C) Examples of lipids showing evident intensity distribution differences between gray and white matter areas of the neocortical section.
BA9 — Brodmann area 9; BA22p — Brodmann area 22 posterior; SM — sphingomyelin; and PC — phosphatidylcholine.
Source: Osetrova et al., 2024.

and more in log-scale. To assess the statistical significance of the difference in the number of lipid changes, the two sample one-sided proportion t-test was used. Pearson's correlation coefficients were calculated on the changes, averaged within lipid classes. To compare the correlation coefficients between the groups, Fisher transformation was applied to Pearson's correlation coefficients, followed by the two-sample one-sided Z-test. The analysis was performed using the R programming language and its publicly available libraries [36]. Analysis results were visualized using the ggplot2 version 3.4.3 package.

Ethical approval

No ethics committee meeting was held. The data provided for the brain samples obtained from National BioService contained no personal information or any other information that could allow donors identification. Informed consent forms for the use of the biomaterial for research purposes were obtained from individuals or from the next-of-kin at the respective clinical organizations that provided the samples to National BioService in accordance with international regulations.

RESULTS

Our analysis of mass spectrometric profiles for BA9 and BA22p derived from over a million pixels across 24 tissue section images yielded intensity data for 153 computational annotations for 131 MALDI peaks detected across the sections, which represented 16 lipid classes (Table S2 and Table S3 in the Supplementary). Clustering analysis of these pixels based on lipid intensities resulted in a reproducible patterning of the neocortical sections into two main areas, which was in alignment with the histologically defined gray and white matter regions, respectively (GM and WM clusters; Figures 1A, 1B). The images generated with specific lipids illustrate differences in distribution across distinct regions (Figure 1C).

In a primary visual cortex study [19], differences in lipid profiles across layers in two neighboring regions, primarily corresponding to a known variation in cortical layer architecture, were described. Visualization of the spatial distribution of two histologically associated lipids from the abovementioned article (SM d42:2, PC 40:6) in our cortical sections indeed revealed specific intensity gradients (Figure 2A). Unsupervised clustering of gray matter resulted in a segmentation of the cortex into three layers (Figure 2B). One-way ANOVA revealed a significant difference in PC 40:6 lipid mean values across the obtained layers for HC both in BA9 (p-value=0.004) and in BA22 (p-value=0.02) and for SZ in BA22 (p-value=0.002), but none in BA9 (p-value=0.1). The number of observations in each comparison was 4 per group.

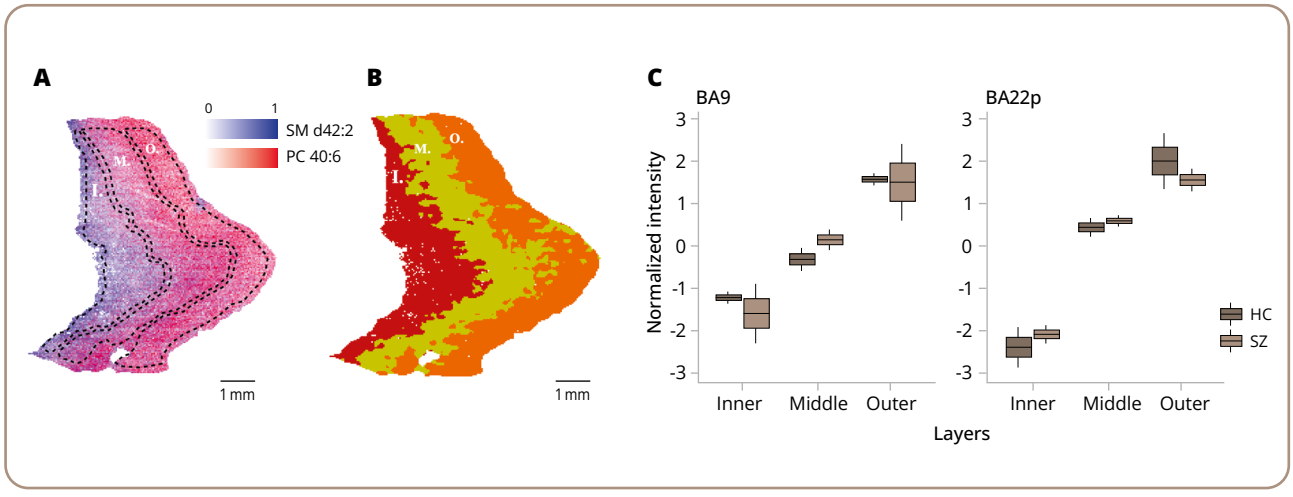

Figure 2. Investigation of the gray matter microstructure.

Note: (A) Superposition of the SM d42:2 and PC 40:6 intensity distribution across the gray matter (I — inner layer, M — middle layer, O — outer layer). (B) Unsupervised clustering of gray matter based on all peaks. (C) Distribution of the cluster mean value of all donors for PC 40:6 [H+] in BA9 and BA22. Color indicates disease. Information presented with a box-plot graph, where the box represents the interquartile range (IQR), with the median marked inside. The whiskers extend to the minimum and maximum values.
BA9 — Brodmann area 9; BA22p — Brodmann area 22 posterior; HC — healthy control; and SZ — schizophrenia patient.
Source: Osetrova et al., 2024.

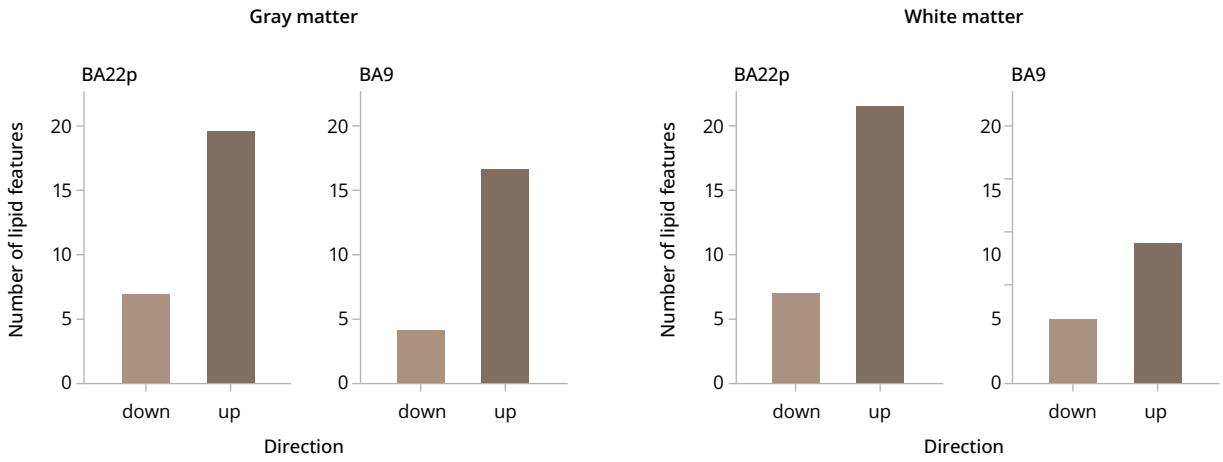

Figure 3. The distribution of lipid differences between the schizophrenia and healthy groups in two specific brain regions.

Note: The boxplots show the number of lipid species that exceeded fold-change thresholds of –0.25 and 0.25 in gray and white matter within the regions of interest (BA9 and BA22p). Lipids with a fold-change range between the –0.25 and 0.25-fold-change distribution are not included in the plot.
BA9 — Brodmann area 9; BA22p — Brodmann area 22 posterior.
Source: Osetrova et al., 2024.

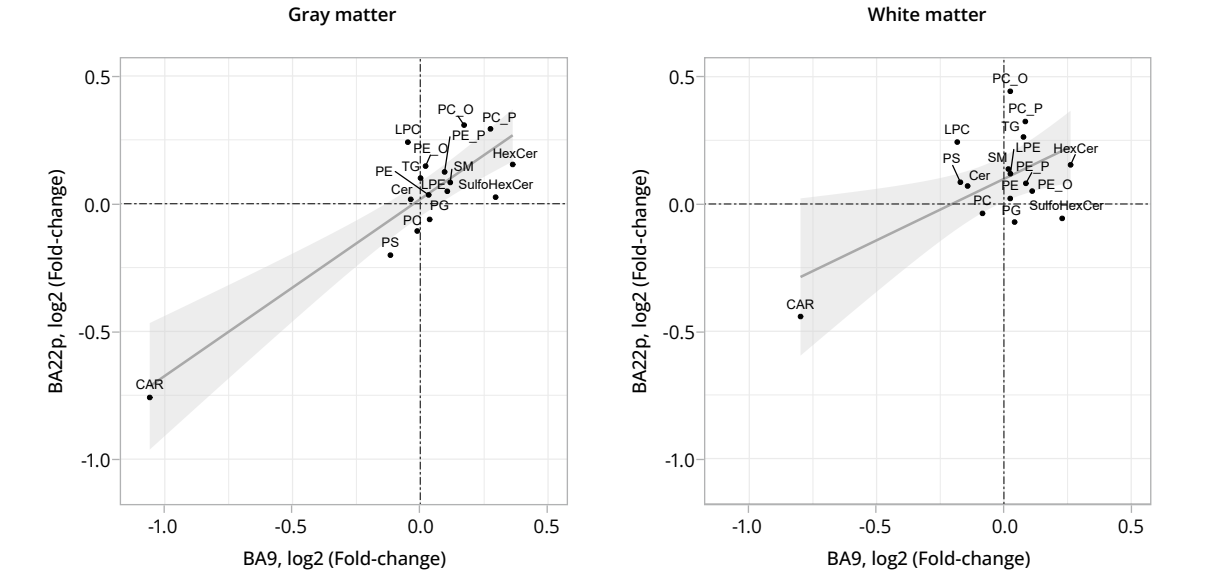

Figure 4. Comparison of the schizophrenia-associated differences detected either in gray or white matter across the two brain regions under investigation.

Note: Each point signifies the average difference (fold-change) in lipid intensity levels between the schizophrenia and control samples, calculated for all lipids within a specific lipid class in either the BA9 (x-axis) or BA22p (y-axis) brain region section. Linear regression lines are drawn with 95% confidence intervals represented by gray shaded areas.
BA9 — Brodmann area 9; BA22p — Brodmann area 22 posterior; SM — sphingomyelin; PC — posphatidylcholine; LPC — lysophosphatidylcholine; CAR — carnitine; PS — phosphoserine; Cer — ceramide; HexCer — hexoceramide; SulfoHexCer — sulfohexoceramide; TG — triglyceride; PC_O and PC_P — ether-linked phosphatidylcholine.
Source: Osetrova et al., 2024.

Analysis of compound intensity differences between the SZ and HC sections using the 131 annotated MALDI peaks yielded twice as many schizophrenia-associated differences in the BA22p region compared to BA9 in the WM: 31 and 17 lipid intensity differences, respectively (one-sided proportion t-test, p=0.019) (Figure 3). However, this disconnect was not statistically significant for the GM, where we had identified 27 and 21 lipid intensity differences, respectively (one-sided proportion t-test, p=0.212) (Figure 3).

In order to directly compare the lipid intensity differences associated with SZ between the two neocortical regions under investigation, we computed and contrasted the average fold-change values for each of the 16 lipid classes within each histological cluster. The differences associated with SZ showed a significant positive correlation between BA22p and BA9 in both the gray matter and white matter areas (Figure 4 and Table S4 in the Supplementary). As predicted from the greater discrepancy between the two brain regions in the number of schizophrenia-affected lipids in the white matter shown in Figure 3, correlation of the schizophrenia-associated differences between BA22p and BA9 in the white matter (Pearson correlation, r=0.57, p=0.017) compared to the gray matter (Pearson correlation, r=0.87, p=0.00001) was also significantly lower (one-sided two-sample Z-test on Fisher transformed Person's R, p=0.040).

Our analysis further highlighted certain lipid classes that demonstrated the most significant amplitude of schizophrenia-associated differences in both neocortical regions. Specifically, acyl-carnitines showed notably lower intensities in both BA22p and BA9 across both histological clusters. If acyl-carnitines were removed from the sample of lipid classes being analyzed, the correlation between regions would decrease in both tissue types, remaining positive and statistically significant for gray matter (Pearson's R=0.49, p=0.03194) and disappearing in the case of white matter (Pearson's R=−0.05, p=0.57).

DISCUSSION

Key results

The present study utilized MALDI-MSI to analyze the cortical sections corresponding to BA22p and BA9 in schizophrenia patients and healthy controls. Our findings suggest that schizophrenia is associated with alterations in lipid composition for the two regions investigated. Notably, we observed approximately twice as many differences in the white matter section of BA22p compared to BA9. This underscores the differential association of schizophrenia in these two functionally and structurally distinct cortical regions. While our results show significant agreement of schizophrenia-associated alterations between the two examined brain regions both in gray and white matter, they also indicate a stronger correlation of schizophrenia-associated differences in the gray matter than in the white matter between these two examined brain areas. This implies that, while the dorsolateral prefrontal cortex (BA9), a commonly investigated region in schizophrenia research, shares most of the schizophrenia-associated alterations with the anatomically distinct temporal lobe region (BA22p), it exhibits fewer differences in the infracortical white matter.

Limitations

Our study had several limitations. First, the number of schizophrenia and control samples used for the analysis was limited to 24, with each condition represented by six samples in each of the two brain regions. Second, our lipid compound annotation was restricted to computational predictions and did not rely on the compound fragmentation spectrum, which would have allowed for more precise identification. Nonetheless, despite these limitations, we observed a positive correlation of schizophrenia-associated differences between two independently measured brain regions. Furthermore, although computational annotation might be imprecise at the individual compound level, it is much more reliable at the lipid class level, as confirmed by the alignment of our results between brain regions. Lastly, our study design did not exclude the potential influence of confounding variables on the lipid composition of the examined brain regions — such as the use of antipsychotic medication, which has been shown to have an impact on the rodent brain [37].

Moreover, due to the limited number of samples analysed in this study, individual effects might interfere with the results, as well as a slight disbalance in sex and age between the two sample sets. However, the fact that the extent of schizophrenia-associated differences in the subcortical white matter of schizophrenia patients is substantially greater in the temporal lobe compared to the prefrontal cortex, while there is no such bias for gray matter, would require an anatomically and histologically dependent effect of these confounding variables on the brain lipidome. This is less likely than a true biological effect, considering previous observations of a higher level

of alterations associated with BA22p in gene expression [29] and structural MRI studies [38].

Interpretation

Our observation of the greater extent of lipidome alterations associated with BA22p aligns well with existing knowledge regarding this region. Numerous neuroimaging studies have previously demonstrated substantial structural abnormalities in the superior temporal gyrus, which encompasses BA22p, in schizophrenia patients [39]. Moreover, variations in the superior temporal gyrus volume have been directly associated with the severity of auditory hallucinations in schizophrenia patients [40–42]. More recently, a study conducted on first-episode treatment-naive schizophrenia patients using structural MRI reported significant alterations in the myelin content in the superior temporal gyrus, but not in the dorsolateral prefrontal cortex [43]. Similarly, molecular studies of BA22 have identified multiple alterations in the transcriptome and proteome in schizophrenia that affect cell adhesion, synaptic transmission, axon guidance, and energy metabolism pathways [26, 44]. Notably, gene expression studies of schizophrenic brains examining 12 and 15 different neocortical regions, including the dorsolateral prefrontal cortex, have consistently found the highest number of alterations in BA22 [29, 45].

Our study aimed to assess whether the lipidome differences associated with schizophrenia, detected in the commonly studied neocortical brain region, BA9, are reflective of the differences present in other neocortical regions. Furthermore, we explored whether incorporating a spatial resolution dimension could reveal additional schizophrenia-associated features within the lipidome alterations. Our findings demonstrate that the spatial lipidomics approach is indeed capable of detecting subtle differences in schizophrenia-associated effects between the two examined higher level association regions of the neocortex. In addition to identifying a generally weaker association of schizophrenia with the white subcortical matter lipid composition of BA9 compared to BA22p, we observed substantial differences in a number of lipid classes with respect to the amplitude of schizophrenia-associated effects between the two regions. Interestingly, the changes were closer for the gray matter clusters of the two investigated regions rather than the white matter ones. Among the most lipid classes with conserved differences for both regions were plasmalogens, previously shown to be associated with schizophrenia in terms of the plasma lipidome [46–48]. Of special interest were acyl-carnitines that demonstrate highly conserved changes with the greatest amplitude in both regions and both types of tissues, being also responsible for the statistically significant correlation in the case of white matter. Schizophrenia patients demonstrated decreased levels for the majority of acyl-carnitines in blood plasma [47, 49], while studies that focused on a brain transcriptome analysis of the dorsolateral prefrontal cortex highlighted acyl-carnitines biosynthesis impairment, as well as an association of changes in the lipid content with cognitive symptoms of schizophrenia [15]. Thus, our results fit into the overall picture of the brain lipid differences associated with schizophrenia.

CONCLUSION

Collectively, our findings suggest that including other neocortical regions beyond the dorsolateral prefrontal cortex into a schizophrenia-associated molecular study might yield promising new insight into the pathology of this disease. Moreover, our results underscore the value of a spatial resolution analysis, which allows for the separation of neocortical sections into gray and white matter areas for data analysis. Through such separation, we were able to identify substantial differences between these two brain regions with respect to schizophrenia-associated alterations in the subcortical white matter, but not in the cortical gray matter. This insight highlights the need for further spatial resolution studies to better understand the molecular alterations associated with complex brain phenotypes such as psychiatric disorders, including schizophrenia.

Article history

Submitted: 11.12.2023
Accepted: 27.08.2024
Published Online: 20.09.2024

Authors' contribution: Methodology, Olga Efimova, Gleb Vladimirov and Elena Stekolschikova; conceptualization, Philipp Khaitovich and Maria Osetrova; software, Maria Osetrova and Pavel Mazin; validation, Maria Osetrova; formal analysis, Maria Osetrova and Marina Zavolskova; investigation, Maria Osetrova and Marina Zavolskova; resources, Olga Efimova, Gleb Vladimirov, George Kostyuk and Evgeniy Nikolaev; data curation, Maria Osetrova, Marina Zavolskova and Elena Stekolschikova; writing original

draft preparation, Maria Osetrova, Marina Zavolskova; writing review and editing, Denis Andreyuk, Yana Zorkina, Anna Morozova and Philipp Khaitovich; visualization, Maria Osetrova and Marina Zavolskova; supervision, Philipp Khaitovich; project administration, Philipp Khaitovich. All authors have read and agreed to the published version of the manuscript.

Funding: Sample collection, measurements, and primary data analysis were funded by the Russian Science Foundation under grant No. 22-15-00474. Data integration analysis was funded by RFBR based on research project No. 20-34-90146.

Conflict of interest: The authors declare no conflicts of interest.

Supplementary data

Supplementary material to this article can be found in the online version:

Figure S1: https://doi.org/10.17816/CP15488-145325

Table S1: https://doi.org/10.17816/CP15488-145326

Table S2: https://doi.org/10.17816/CP15488-145327

Table S3: https://doi.org/10.17816/CP15488-145328

Table S4: https://doi.org/10.17816/CP15488-145329

For citation:

Osetrova MS, Zavolskova MD, Mazin PV, Stekolschikova EA, Vladimirov GN, Efimova OI, Morozova AY, Zorkina YA, Andreyuk DS, Kostyuk GP, Nikolaev EN, Khaitovich PhE. Mass spectrometry imaging of two neocortical areas reveals the histological selectivity of schizophrenia-associated lipid alterations. *Consortium Psychiatricum*. 2024;5(3):CP15488. doi: 10.17816/CP15488

Information about the authors

***Maria Stanislavovna Osetrova**, engineer researcher, V. Zelman Center for Neurobiology and Brain Restoration, Skolkovo Institute of Science and Technology; e-Library SPIN-code: 5813-1688, Scopus Author ID: 57505703600, Researcher ID: HOH-3453-2023, ORCID: https://orcid.org/0000-0002-8174-9544
E-mail: maria.osetrova.sk@gmail.com

Marina Dmitrievna Zavolskova, Junior Researcher, V. Zelman Center for Neurobiology and Brain Restoration, Skolkovo Institute of Science and Technology; e-Library SPIN-code: 1800-6986, Scopus Author ID: 57209106743, ORCID: https://orcid.org/0000-0003-4532-0721

Pavel Vladimirovich Mazin, Cand. Sci (Biolog.), Senior bioinformatician, Wellcome Sanger Institute; e-Library SPIN-code: 2062-8545, Scopus Author ID: 20734870400, ORCID: https://orcid.org/0000-0001-9268-3352

Elena Alekseevna Stekolschikova, Cand. Sci (Chem.), Senior Researcher, V. Zelman Center for Neurobiology and Brain Restoration, Skolkovo Institute of Science and Technology; e-Library SPIN-code: 3859-4534, Scopus Author ID: 56462907300, Researcher ID: U-1735-2018, ORCID: https://orcid.org/0000-0001-8607-9773

Gleb Nikolaevich Vladimirov, Cand. Sci (Phys. and Math.), Senior Researcher, V. Zelman Center for Neurobiology and Brain Restoration, Skolkovo Institute of Science and Technology; Scopus Author ID: 55579659300, ORCID: https://orcid.org/0000-0003-4623-4884

Olga Igorevna Efimova, Junior Research Scientist, V. Zelman Center for Neurobiology and Brain Restoration, Skolkovo Institute of Science and Technology; e-Library SPIN-code: 3427-8085, Scopus Author ID: 15836570500, ORCID: https://orcid.org/0000-0003-0842-3203

Anna Yurievna Morozova, MD, Cand. Sci (Med.), Senior Researcher, Mental-health clinic No. 1 named after N.A. Alexeev; V. Serbsky National Medical Research Centre of Psychiatry and Narcology of the Ministry of Health of the Russian Federation; e-Library SPIN-code: 3233-7638, Researcher ID: T-1361-2019, Scopus Author ID: 55648593900, ORCID: https://orcid.org/0000-0002-8681-5299

Yana Alexandrovna Zorkina, Cand. Sci (Biolog.), Senior Researcher, Mental-health clinic No. 1 named after N.A. Alexeev; V. Serbsky National Medical Research Centre of Psychiatry and Narcology of the Ministry of Health of the Russian Federation; e-Library SPIN-code: 3017-3328, Researcher ID: H-2424-2013, Scopus Author ID: 54584719100, ORCID: https://orcid.org/0000-0003-0247-2717

Denis Sergeevich Andreyuk, Cand. Sci (Biolog.), Mental-health clinic No. 1 named after N.A. Alexeev; Researcher ID: AAQ-6260-2020, Scopus Author ID: 6602608643, ORCID: https://orcid.org/0000-0002-3349-5391

George Petrovich Kostyuk, MD, Dr. Sci (Med.), Professor, Head of Mental-health clinic No. 1 named after N.A. Alexeev; e-Library SPIN-code: 3424-4544, Researcher ID: AAA-1682-2020, Scopus Author ID: 57200081884, ORCID: https://orcid.org/0000-0002-3073-6305

Evgeniy Nikolaevich Nikolaev, Cand. Sci (Biolog.), Professor, Head of the Mass Spectrometry Laboratory, Center for Molecular and Cellular Biology, Skolkovo Institute of Science and Technology; e-Library SPIN-code: 4984-1007, Scopus Author ID: 55394217800, ORCID: https://orcid.org/0000-0001-6209-2068

Philipp Efimovich Khaitovich, Cand. Sci (Biolog.), Professor, Director of the V. Zelman Center for Neurobiology and Brain Restoration, Skolkovo Institute of Science and Technology; Scopus Author ID: 6602559039, ORCID: https://orcid.org/0000-0002-4305-0054

*corresponding author

References

1. Sontheimer H. Chapter 13 – Schizophrenia. In: Sontheimer H, editor. Diseases of the Nervous System. San Diego: Academic Press; 2015. p. 375–403.
2. He H, Liu Q, Li N, et al. Trends in the incidence and DALYs of schizophrenia at the global, regional and national levels: results from the Global Burden of Disease Study 2017. Epidemiol Psychiatr Sci. 2020;29:e91. doi: 10.1017/S2045796019000891
3. Subramaniam M, Abdin A, Vaingankarm JA, et al. Lifetime Prevalence and Correlates of Schizophrenia and Other Psychotic Disorders in Singapore. Front Psychiatry. 2021;12:650674. doi: 10.3389/fpsyt.2021.650674
4. International Journal of Scientific Research [Internet]. Available from: https://www.worldwidejournals.com/international-journal-of-scientific-research-(IJSR)
5. Zhu X, Xu T, Peng C, et al. Advances in MALDI Mass Spectrometry Imaging Single Cell and Tissues. Front Chem. 2021;9:782432. doi: 10.3389/fchem.2021.782432

6. Longuespée R, Casadonte R, Kriegsmann M, et al. ALDI mass spectrometry imaging: A cutting-edge tool for fundamental and clinical histopathology. Proteomics Clin Appl. 2016;10(7):701–719. doi: 10.1002/prca.201500140
7. Liu D, Liu X, Huang S, et al. Simultaneous Mapping of Amino Neurotransmitters and Nucleoside Neuromodulators on Brain Tissue Sections by On-Tissue Chemoselective Derivatization and MALDI-MSI. Anal Chem. 2023:95(45):16549–16557. doi: 10.1021/acs.analchem.3c0267
8. Matsumoto J, Sugiura Y, Yuki D, et al. Abnormal phospholipids distribution in the prefrontal cortex from a patient with schizophrenia revealed by matrix-assisted laser desorption/ ionization imaging mass spectrometry. Anal Bioanal Chem. 2011;400(7):1933–1943. doi: 10.1007/s00216-011-4909-3
9. Kakuda N, Miyasaka T, Iwasaki N, et al. Distinct deposition of amyloid-β species in brains with Alzheimer's disease pathology visualized with MALDI imaging mass spectrometry. Acta Neuropathol Commun. 2017;5(1):73. doi: 10.1186/s40478-017-0477-x
10. Smith A, L'Imperio V, Ajello E, et al. The putative role of MALDI-MSI in the study of Membranous Nephropathy. Biochim Biophys Acta Proteins Proteomics. 2017;1865(7):865–874. doi: 10.1016/j.bbapap.2016.11.013
11. Lim J, Aguilan JT, Sellers RS, et al. Lipid mass spectrometry imaging and proteomic analysis of severe aortic stenosis. J Mol Histol. 2020;51(5):559–571. doi: 10.1007/s10735-020-09905-5
12. Wang D, Sun X, Maziade M, et al. Characterising phospholipids and free fatty acids in patients with schizophrenia: A case-control study. World J Biol Psychiatry. 2021;22(3):161–174. doi: 10.1080/15622975.2020.1769188
13. Yu Q, He Z, Zubkov D, et al. Lipidome alterations in human prefrontal cortex during development, aging, and cognitive disorders. Mol Psychiatry. 2020;25(11):2952–2969. doi: 10.1038/s41380-018-0200-8
14. Ghosh S, Dyer RA, Beasley CL. Evidence for altered cell membrane lipid composition in postmortem prefrontal white matter in bipolar disorder and schizophrenia. J Psychiatr Res. 2017;95:135–142. doi: 10.1016/j.jpsychires.2017.08.009
15. Maas DA, Martens MB , Nikos Priovoulos N, et al. Key role for lipids in cognitive symptoms of schizophrenia. Transl Psychiatry. 2020;10(1):399. doi: 10.1038/s41398-020-01084-x
16. Shimamoto-Mitsuyama C, Nakaya A, Esaki K, et al. Lipid Pathology of the Corpus Callosum in Schizophrenia and the Potential Role of Abnormal Gene Regulatory Networks with Reduced Microglial Marker Expression. Cereb Cortex. 2021;31(1):448–462. doi: 10.1093/cercor/bhaa236
17. Huang S, Wu SJ, Sansone G, et al. Layer 1 neocortex: Gating and integrating multidimensional signals. Neuron. 2024;112(2):184–200. doi: 10.1016/j.neuron.2023.09.041
18. Larkum ME, Petro LS, Sachdev RNS, et al. Perspective on Cortical Layering and Layer-Spanning Neuronal Elements. Front Neuroanat. 2018;12:56. doi: 10.3389/fnana.2018.00056
19. González de San Román E, Bidmon HJ, Malisic M, et al. Molecular composition of the human primary visual cortex profiled by multimodal mass spectrometry imaging. Brain Struct Funct. 2018;223(6):2767–2783. doi: 10.1007/s00429-018-1660-y
20. Smucny J, Hanks TD, Lesh TA, et al. Altered Associations Between Task Performance and Dorsolateral Prefrontal Cortex Activation During Cognitive Control in Schizophrenia. Biol Psychiatry Cogn Neurosci Neuroimaging. 2023;8(10):1050–1057. doi: 10.1016/j.bpsc.2023.05.010
21. Meiron O, Yaniv A, Rozenberg S, et al. Transcranial direct-current stimulation of the prefrontal cortex enhances working memory and suppresses pathological gamma power elevation in schizophrenia. Expert Rev Neurother. 2024;24(2):217–226. doi: 10.1080/14737175.2023.2294150
22. Gan H, Zhu J, Zhuo K, et al. High frequency repetitive transcranial magnetic stimulation of dorsomedial prefrontal cortex for negative symptoms in patients with schizophrenia: A double-blind, randomized controlled trial. Psychiatry Res. 2021;299:113876. doi: 10.1016/j.psychres.2021.113876
23. Smucny J, Carter CS, Maddock RJ. Magnetic resonance spectroscopic evidence of increased choline in the dorsolateral prefrontal and visual cortices in recent onset schizophrenia. Neurosci Lett. 2022;770:136410. doi: 10.1016/j.neulet.2021.136410
24. Shi C, Yu X, Cheung EFC, et al. Revisiting the therapeutic effect of rTMS on negative symptoms in schizophrenia: a meta-analysis. Psychiatry Res. 2014;215(3):505–513. doi: 10.1016/j.psychres.2013.12.019
25. Levitan C, Ward PB, Catts SV. Superior temporal gyral volumes and laterality correlates of auditory hallucinations in schizophrenia. Biol Psychiatry. 1999;46(7):955–962. doi: 10.1016/s0006-3223(98)00373-4
26. Barnes MR, Huxley-Jones J, Maycox PP, et al. Transcription and pathway analysis of the superior temporal cortex and anterior prefrontal cortex in schizophrenia. J Neurosci Res. 2011;89(8):1218–1227. doi: 10.1002/jnr.22647
27. Huang KC, Yang KC, Lin H, et al. Transcriptome alterations of mitochondrial and coagulation function in schizophrenia by cortical sequencing analysis. BMC Genomics. 2014;15(Suppl 9):S6. doi: 10.1186/1471-2164-15-S9-S6
28. Dienel SJ, Fish KN, Lewis DA. The Nature of Prefrontal Cortical GABA Neuron Alterations in Schizophrenia: Markedly Lower Somatostatin and Parvalbumin Gene Expression Without Missing Neurons. Am J Psychiatry. 2023;180(7):495–507. doi: 10.1176/appi.ajp.20220676
29. Katsel P, Davis KL, Haroutunian V. Variations in myelin and oligodendrocyte-related gene expression across multiple brain regions in schizophrenia: a gene ontology study. Schizophr Res. 2005;79(2–3):157–173. doi: 10.1016/j.schres.2005.06.007
30. Bemis KD, Harry A, Eberlin LS, et al. Cardinal: an R package for statistical analysis of mass spectrometry-based imaging experiments. Bioinformatics. 2015;31(14):2418–2420. doi: 10.1093/bioinformatics/btv146
31. McMillen JC, Fincher JA, Klein DR, et al. Effect of MALDI matrices on lipid analyses of biological tissues using MALDI-2 postionization mass spectrometry. J Mass Spectrom. 2020;55(12):e4663. doi: 10.1002/jms.4663
32. Monopoli A, Ventura G, Aloia A, et al. Synthesis and Investigation of Novel CHCA-Derived Matrices for Matrix-Assisted Laser Desorption/Ionization Mass Spectrometric Analysis of Lipids. Molecules. 2022;27(8):2565. doi: 10.3390/molecules27082565.
33. Dufresne M, Fisher JA, Patterson NH, et al. α-Cyano-4-hydroxycinnamic Acid and Tri-Potassium Citrate Salt Pre-Coated Silicon Nanopost Array Provides Enhanced Lipid Detection for High Spatial Resolution MALDI Imaging Mass Spectrometry. Anal Chem. 2021;93(36):12243–12249. doi: 10.1021/acs.analchem.1c01560
34. Thomas A, Charbonneau JL, Fournaise E, et al. Sublimation of new matrix candidates for high spatial resolution imaging mass spectrometry of lipids: enhanced information in both positive and negative polarities after 1,5-diaminonapthalene deposition. Anal Chem. 2012;84(4):2048–2054. doi: 10.1021/ac2033547

35. Angerer TB, Bour J, Biagi JL, et al. Evaluation of 6 MALDI-Matrices for 10 µm Lipid Imaging and On-Tissue MSn with AP-MALDI-Orbitrap. J Am Soc Mass Spectrom. 2022;33(5):760–771. doi: 10.1021/jasms.1c00327
36. Ripley BD. The R project in statistical computing. MSOR Connect. 2001;1(1):23–25. doi: 10.11120/MSOR.2001.01010023
37. Zhou CH, Xue SS, Xue F, et al. The impact of quetiapine on the brain lipidome in a cuprizone-induced mouse model of schizophrenia. Biomed Pharmacother. 2020;131:110707. doi: 10.1016/j.biopha.2020.110707
38. Honea R, Crow TJ, Passingham D, et al. Regional deficits in brain volume in schizophrenia: a meta-analysis of voxel-based morphometry studies. Am J Psychiatry. 2005;162(12):2233–2245. doi: 10.1176/appi.ajp.162.12.2233
39. Zhao J, Zhang Y, Liu F, et al. Abnormal global-brain functional connectivity and its relationship with cognitive deficits in drug-naive first-episode adolescent-onset schizophrenia. Brain Imaging Behav. 2022;16(3):1303–1313. doi: 10.1007/s11682-021-00597-3
40. Shen X, Jiang F, Fang X, et al. Cognitive dysfunction and cortical structural abnormalities in first-episode drug-naïve schizophrenia patients with auditory verbal hallucination. Front Psychiatry. 2022;13:998807. doi: 10.3389/fpsyt.2022.998807
41. Ysbæk-Nielsen AT, Gogolu RF, Tranter M, et al. Structural brain abnormalities in patients with schizophrenia spectrum disorders with and without auditory verbal hallucinations. Psychiatry Res Neuroimaging. 2024;344:111863. doi: 10.1016/j.pscychresns
42. Zhang M, Xiang H, Yang F, et al. Structural brain imaging abnormalities correlate with positive symptom in schizophrenia. Neurosci Lett. 2022;782:136683. doi: 10.1016/j.neulet.2022.136683
43. Wei W, Zhang Y, Li Y, et al. Depth-dependent abnormal cortical myelination in first-episode treatment-naïve schizophrenia. Hum Brain Mapp. 2020;41(10):2782–2793. doi:10.1002/hbm.24977
44. Martins-de-Souza D, Gattaz WF, Schmitt A, et al. Proteome analysis of schizophrenia patients Wernicke's area reveals an energy metabolism dysregulation. BMC Psychiatry. 2009;9:17. doi: 10.1186/1471-244X-9-17
45. Katsel PL, Davis KL, Haroutunian V. Large-scale microarray studies of gene expression in multiple regions of the brain in schizophrenia and Alzheimer's disease. Int Rev Neurobiol. 2005;63:41–82. doi: 10.1016/S0074-7742(05)63003-6
46. Kaddurah-Daouk R, McEvoy J, Baillie R, et al. Impaired plasmalogens in patients with schizophrenia. Psychiatry Res. 2012;198(3): 347–352. doi: 10.1016/j.psychres.2012.02.019
47. Cao B, Wang D, Pan Z, et al. Characterizing acyl-carnitine biosignatures for schizophrenia: a longitudinal pre- and post-treatment study. Transl Psychiatry. 2019;9(1):19. doi: 10.1038/s41398-018-0353-x
48. Mednova IA, Chernonosov AA, Kornetova EG, et al. Levels of Acylcarnitines and Branched-Chain Amino Acids in Antipsychotic-Treated Patients with Paranoid Schizophrenia with Metabolic Syndrom. Metabolites. 2022;12(9). doi: 10.3390/metabo12090850
49. Mednova IA, Chernonosov AA , Kasakin MF, et al. Amino Acid and Acylcarnitine Levels in Chronic Patients with Schizophrenia: A Preliminary Study. Metabolites. 2021;11(1):34. doi: 10.3390/metabo11010034